Unique Calibrators Derived from Fluorescence-Activated Nanoparticle Sorting for Flow Cytometric Size Estimation of Artificial Vesicles: Possibilities and Limitations

Simonsen, Jens B.; Larsen, Jannik B.; Hempel, Casper; Eng, Niklas; Fossum, Anna; Andresen, Thomas L.

Published in:
Cytometry. Part A

Link to article, DOI:
10.1002/cyto.a.23797

Publication date:
2019

Document Version
Peer reviewed version

Cytometry PART A
ISAC
Journal of Quantitative Cell Science

Unique Calibrators Derived from Fluorescence-Activated Nanoparticle Sorting for Flow Cytometric Size Estimation of Artificial Vesicles: Possibilities and Limitations

Jens B. Simonsen,[1*] Jannik B. Larsen,[1] Casper Hempel,[1] Niklas Eng,[2] Anna Fossum,[3] Thomas L. Andresen[1]

[1]Department of Health Technology, Technical University of Denmark, Kongens Lyngby DK-2800, Denmark

[2]Teamator AB, SE-25023 Helsingborg, Sweden

[3]Biotech Research and Innovation Centre (BRIC), University of Copenhagen, Copenhagen DK-2200, Denmark

Received 24 October 2018; Revised 8 April 2019; Accepted 6 May 2019

Grant sponsor: Det Frie Forskningsråd; Grant sponsor: Lundbeckfonden, Grant number: R155-2013-14113; Grant sponsor: Novo Nordisk Foundation, Grant numbers: NNF16OC0022166, NNF17OC0028262

Additional Supporting Information may be found in the online version of this article.

*Correspondence to: Jens B. Simonsen, Produktionstorvet, Building 423, DK-2800 Kgs. Lyngby, Denmark.
Email: jbak@dtu.dk

Published online in Wiley Online Library (wileyonlinelibrary.com)

DOI: 10.1002/cyto.a.23797

Abstract

The use of high-throughput flow cytometry to characterize nanoparticles has received increased interest in recent years. However, to fully realize the potential of flow cytometry for the characterization of nanometer-sized objects, suitable calibrators for size estimation must be developed and the sensitivity of conventional flow cytometers has to be advanced. Based on the scattered signal, silica and plastic beads have often been used as flow cytometric size calibrators to evaluate the size of extracellular vesicles and artificial vesicles (liposomes). However, several studies have shown that these beads are unable to accurately correlate scatter intensity to vesicle size. In this work, we present a novel method to estimate the size of individual liposomes in flow cytometry based on liposomal size calibrators prepared by fluorescence-activated cell sorting (FACS), here coined fluorescence-activated nanoparticle sorting (FANS). These calibration liposomes exhibit sizes, structures, and refractive indexes identical to the particles being studied and thus can serve as unique calibrators. First, a sample of polydisperse fluorophore-labeled unilamellar liposomes was prepared and analyzed by flow cytometry. Next, different fractions of the polydisperse liposomes were FANS-sorted according to their fluorescence intensity. Thereafter, we employed nanoparticle tracking analysis (NTA) to evaluate the liposome sizes of the FANS-sorted liposome fractions. Finally, we correlated the flow cytometric readouts (side scatter and fluorescence intensity) of the FANS-sorted liposome fractions with their corresponding size obtained by NTA. This procedure enabled us to translate the liposome fluorescence intensity to the liposome size in nanometers for all detected individual liposomes. We validated the size distribution of our polydisperse liposome sample obtained from flow cytometry in combination with our FANS-calibrators against standard methods for sizing nanoparticles, including NTA and cryo-transmission electron microscopy. This work also highlights the limitation of using the flow cytometric side scattering readout to determine the size of small (30–300 nm) artificial vesicles. © 2019 International Society for Advancement of Cytometry

Key terms

calibrators; size; flow cytometry; sorting; FACS; FANS; NTA; nanoparticles; liposomes; extracellular vesicles

To be able to analyze multiple parameters of individual nanoparticles, including their size, in a high-throughput manner has long been a goal in nanoparticle research. Traditional tools for nanoparticle characterization are often limited by a low throughput, such as microscopy-based methods, or restricted to single-property measurements using ensemble-based methods. The potential problem with employing bulk absorption and emission spectroscopy-based methods or dynamic light small-angle X-ray or neutron scattering techniques is that the ensemble average information they provide

may not always reflect the actual properties of the individual objects of the sample—especially in cases of highly heterogeneous nanoparticle samples. High-throughput flow cytometry has proven to be very efficient in providing multifaceted information about biochemical attributes and relative sizes of individual cells. However, as these conventional flow cytometry setups were originally designed to probe micrometer-sized biological objects, they are challenged when it comes to studying nanoparticles with a size range two orders of magnitude smaller.

Only recently has the ability of flow cytometry been explored and exploited to also include the characterization of nanoparticles. A few studies have employed flow cytometry to study nanoparticles made of polystyrene, silica, titanium dioxide, gold, or silver (1–3). Artificial vesicles (liposomes) have also been studied (4–8), but the focus has largely been on assessing the enumeration, surface antigens, and size distributions of biological nano-sized vesicles known as extracellular vesicles (EVs) (8–15). The emerging research field of EV biology has largely been driven by the potential to use EVs as disease biomarkers (16) or as targeted drug delivery vehicles (17). However, the small difference in refractive index between vesicles and water as well as the typical small size of vesicles hamper the accurate detection and quantitative analyzes of these dim particles by flow cytometry.

To harness the full potential of flow cytometry for characterizing the size and chemical composition of low refractive index nanoparticles, two fundamental improvements are needed. First, the detection sensitivity of conventional flow cytometers has to be improved. Several efforts are ongoing in this field and recently Zhu et al. (2) showed that a unique home-built flow cytometer could detect 7 nm-sized gold nanoparticles, whereas Nolan et al. (8) demonstrated that a laboratory-built flow cytometric setup was capable of detecting artificial and biological vesicles down to about 80 nm. These improvements were obtained by increasing the exposure time (by decreasing the flow rate of the sheath fluid), increasing the laser power, and improving the system optics. The second area of improvement is the development of proper size calibrators, because flow cytometry does not provide direct information about size. These calibrators will ideally be very similar to or identical to the nanoparticles that are under investigating, allowing the conversion of the scattering or emission readouts to actual physical size. Plastic and silica beads have previously been used as calibrators to determine the size of liposomes (5,6) based on the flow cytometric scattering output, but recent studies (4,13) suggest that using such beads may be problematic due to their higher refractive index compared to liposomes and EVs, leading to errors in size calibration. A theoretical approach based on Mie scattering theory has also been applied to assign sizes to EVs based on their scattering intensity (12,13). However, the call for bona fide size-calibrator standards is continuously emphasized by the flow cytometry community (14,18–20).

This work presents a novel approach for creating, evaluating, and employing flow cytometric size calibrators with sizes, structures, and refractive indexes that are identical to the nanoparticles being studied. We used fluorescence-activated nanoparticle sorting (here coined FANS) of fluorophore-labeled liposomes to create differentially sized liposome calibrators and determined the size of these FANS-sorted liposomes by using nanoparticle tracking analysis (NTA). Next, we correlated liposome size with both scatter and fluorescence intensity by using the FANS-sorted calibrators. Finally, we validated the size distribution of a polydisperse fluorophore-labeled liposome sample derived from the flow cytometric fluorescent readout in combination with our FANS-sorted calibrators against standard methods for sizing nanoparticles including NTA and cryo-TEM.

Materials and Methods

Preparation of Unilamellar Liposomes

We prepared unilamellar liposomes by the standard lyophilization method (21) using the following lipid composition: 1% (by mole) 1,2-dioleoyl-sn-glycero-3-phosphoethanol-amine)-atto488 (DOPE-atto488), 10% 1-palmitoyl-2-oleoyl-sn-glycero-3-phospho-L-serine (POPS) and 89% 1-palmitoyl-2-oleoyl-sn-glycero-3-phosphocholine (POPC). POPC and POPS were purchased from Sigma-Aldrich and DOPE-atto488 was purchased from ATTO-TEC GmbH as powders. All lipids were dissolved in *tert*-butanol and mixed according to the composition described earlier, frozen in liquid nitrogen, and dried overnight. The lyophilized lipid mixture (1 mg) was fully hydrated in 1 ml of 285 mM sorbitol solution prepared from MilliQ water by incubation at room temperature overnight. Then, the liposome solution went through 10 freeze/thaw cycles followed by a single extrusion through an 800 nm sized pore membrane (isopore polycarbonate membranes from Millipore) using an Avanti Mini-extruder. Prior to the flow cytometry measurements, the liposomes in sorbitol were diluted by a factor of ~8,000 in a standard Dulbecco's phosphate-buffered saline (DPBS) sheath fluid (Invitrogen, Life Technologies). The sorbitol and DPBS solutions used for lipid resuspension and dilution, respectively, were filtered through a standard 0.22 μm filter prior to use. The total molarity of the sorbitol solution the liposomes were formed in was identical to the DPBS buffer to avoid osmotic stress on the liposomes and to slightly enhance the difference between the refractive index of the liposomes interior and the DPBS solvent.

Fluorescence-Activated Nanoparticle Sorting

We used a FACSAria (BD Biosciences) to sort and study our liposomes. BD CS&T quality and control beads were used prior to the experiments to standardize the performance of the FACSAria. An approximately 8,000-fold dilution of the liposomes along with a low flow rate (1 μl/min) enabled us to avoid co-particle events according to the linear relation between the count rate and the corresponding dilution and the fairly constant mean fluorescence intensity (see Fig. S1 in the Supporting Information). The events (~2,000–3,000 events/s) were triggered by the fluorescence from DOPE-atto488 at the lowest fluorescence intensity at which almost no events (count rate <2/s) were detected from the bare DPBS to discriminate

fluorophore-labeled liposomes from the background. The liposomes were sorted using the following fluorescence-based gatings: 296–394, 692–894, and 995–1,245. The liposomes were sorted into Falcon round-bottom polystyrene tubes from BD Biosciences. We learned that low-protein-binding Eppendorf tubes gave rise to a large shift in FI compared to the sorting gates. A 70 µm nozzle was used for the sorting that gives rise to a final particle concentration of the sorted fractions of about 10^6 particles/ml. The atto488 emission was detected by a detector with a detection range of 502–550 nm. The applied voltages for the fluorescence and SSC channels were 550 and 900 V, respectively. The fluorescence trigger (threshold) value was set to 200. The SSC and fluorescence readouts were based on the height signal of the recorded pulses. We recorded 100,000 events for bulk (polydisperse) liposome analysis and 10,000 for the sorted liposome fractions (Fig. 1). We reduced the fluorescence intensity data into 50 equally sized bins (in log scale) in the range from 100 to 100,000. Our approach is independent on the scale of fluorescence, because we are sorting according to relative fluorescence intensities. However, to be able to compare data between experiments, we also transformed the fluorescence data shown in Figure 1B to alexa488 MESF standard values by using Quantum™ Alexa488 Fluor® MESF beads purchased from Polysciences. The fluorescence intensities from the differently labeled quantum beads and the corresponding standard curve used for the alexa488 MESF transformation were obtained using a standard protocol and the data are shown in the Supporting Information Figure S2A and B. The alexa488 MESF transformed data are shown in the Supporting Information Figure S2C. The SSC data were reduced into 50 equally sized bins in the linear range from 100 to 5,000. The SSC profile from the bare DPBS was only based on 500 events due to the slow event rate. The binned DPBS data were scaled with a factor of 20 for better visualization in Figure 5. We used Origin® for data binning, analysis, and plots. The SSC-FI density plot insert in Figure 1B and the Supporting Information Figure S4 were performed using FlowJo®. We reported the SSC signal rather the forward scattering (FSC) readout because the sensitivity of the SSC is traditionally higher than that of the FSC signal in the case of conventional BD flow cytometry equipment. Moreover, we chose to report the height value from the SSC recording because it has been reported to be the optimal readout when studying small dim scatters (11).

Nanoparticle Tracking Analysis

NTA was used to estimate the liposome size of the different FANS-sorted fractions. This technique infers size from the Brownian motions of individual particles and thus complements size determination based on scattering and fluorescence detection. The motion of the particles can be tracked by either scattered light or fluorescence. The ZetaView from Particle Metrix (NTA) equipped with a 488 nm laser and a CCD camera was calibrated against 100 nm beads from Microtrac Inc. prior to the liposome measurements. The temperature in the chamber was fixed at 25°C. The unsorted liposome sample was diluted in filtered DPBS before loading, while the sorted fractions were loaded directly into the chamber. The minimum brightness was set to 20 (minimum size 5 nm and maximum size 1,000 nm) and a trace length of 15 frames, camera sensitivity of 95, duration of 0.5 or 2 s, and shutter times of 62 or 70 ms were used. The liposomes were detected in fluorescence mode to avoid background events. Seven to 14 cycles of 30 or 60 s each were recorded and analyzed for each sample using the ZetaView 8.04.02 software.

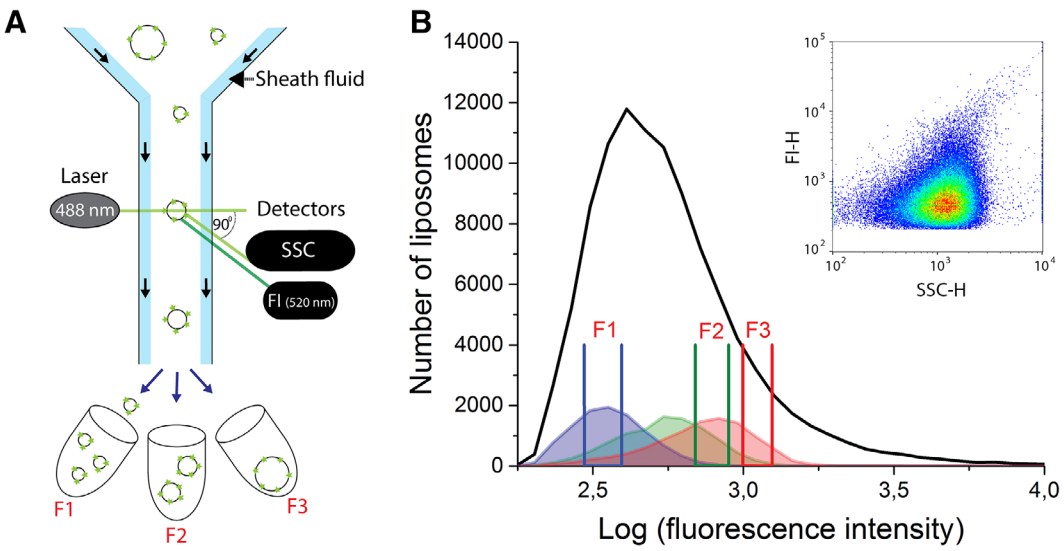

Figure 1. (**A**) Schematic illustration of a flow cytometer including the FANS-sorting feature. (**B**) Histograms based on the fluorescence intensity (*FI*) from the bulk (polydisperse) liposome solution (black line) used for liposome sorting, the gates used for sorting liposomes (colored lines) and the reanalyzed sorted liposome fractions (solid colors). The insert in B shows the *FI-H*/SSC-*H* 2D-density plot of the bulk (polydisperse) liposome solution. The 2D-density plots of the sorted fractions are shown in the Supporting Information (Fig. S4).

Cryo-Transmission Electron Microscopy

Samples were loaded on lacey carbon-coated grids and plunge frozen in liquid nitrogen-cooled liquid ethane by using a Vitrobot (FEI, OR, US). The vitrified samples were loaded into a Tecnai G2 Twin microscope (Fei) and imaged at low dose to reduce beam damage. Liposome diameter was measured by using Fiji (22).

Results

Empty Unilamellar Liposomes

To correlate fluorescence intensity or SSC readouts to the size of the individual liposomes, it was a prerequisite that we could form empty (without encapsulated liposomes) unilamellar (as opposed to multilamellar) liposomes. We explicitly employed a rehydration sorbitol-solution without salt during the liposome formation of the negatively charged liposomes (10 mol% POPS) to promote the formation of unilamellar liposomes (23,24). Cryo-TEM studies confirmed that all liposomes were unilamellar and more than 94% were empty. Representative Cryo-TEM micrographs are shown in the Supporting Information Figure S3.

Fluorescence-Activated Nanoparticle Sorting

For our flow cytometric studies, we used the 488 nm laser and detected SSC at 488 nm and fluorescence from the DOPE-atto488 (setup shown in Fig. 1A). The presence of DOPE-atto488, a lipid-anchored fluorophore, in our liposomes enabled us to trigger flow cytometric events based on fluorescence thereby avoiding recording events from artifacts. The flow cytometric fluorescence intensity profile of the bulk (polydisperse) liposome sample is shown in Figure 1B. We decided to FANS-sort the bulk liposome sample into three distinct populations (F1, F2, and F3) according to their fluorescence intensity using the gates shown in Figure 1B. Next, the sorted liposome fractions were reanalyzed by flow cytometry under the same settings, revealing that 15–40% of the sorted liposome populations fall within their respective sorting gates (Fig. 1B). The profiles of the FANS-sorted liposomes are centered close to the sorting cut-off that shows the highest liposome frequency in the whole population—meaning fraction F1 is shifted to the right while fraction F2 and F3 are shifted to the left.

Size Determination Based on NTA

The sorting based on a 70 µm nozzle (as is the case for conventional FACS machines) produces samples with a particle concentration of about 10^6 particles/ml corresponding to a molar particle concentration of about 10^{-15} M. The low concentration of sorted liposome means that any subsequent analysis is limited to measurement setups with high detection sensitivity. The NTA tool is capable of measuring concentrations down to 10^6 nanoparticles/ml. For this reason, we chose to use NTA to size the FANS-sorted liposomes. We decided, like in the case of our FANS-sorting, to trigger the NTA events on fluorescence rather than the light scattering to avoid nonliposomal events, triggered by air bubbles or other

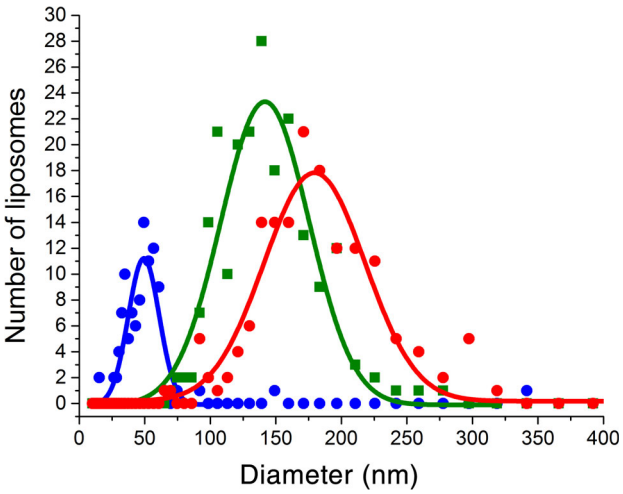

Figure 2. NTA-based size distributions of the sorted liposome fractions F1 (blue solid circles, 104 events), F2 (green solid squares, 211 events), and F3 (red solid circles, 155 events) including their corresponding Gaussian fits (solid lines). The NTA data were recorded in fluorescence mode.

scattering artifacts. The NTA data were fitted with a Gaussian function (Fig. 2). This resulted in sizes of 49 ± 12 nm, 142 ± 34 nm, and 180 ± 39 nm for F1, F2, and F3, respectively. The reported values from NTA of the three different sorted liposome fractions represent the mean value and standard deviations (*SD*) obtained from Gaussian fits.

Correlating the Fluorescence of Liposomes with Size

To correlate the fluorescence intensity with liposome size, we plotted the mean value derived from the Gaussian analysis of the fluorescence intensity data shown in Figure 3A as a function of the corresponding mean value derived from the Gaussian analysis of the NTA data (Fig. 2). This was performed for each of the three sorted samples (Fig. 3B).

The relation between size (diameter, *D*) and fluorescence intensity (FI) follows the relation $D(\mathrm{FI}) = \sqrt{((\mathrm{FI}-b)/k)}$ (25), meaning that the fluorescence intensity scales with the area of the liposome and thus the diameter is proportional to the square root of FI. A background (*b*, including detector noise) and a calibration factor (*k*) are also included in the formula.

The data for NTA-derived diameters of the three FANS-sorted size populations (Fig. 2) as a function of their corresponding *FI* (Fig. 3A) appear to follow the expected *D*(FI)-relation (25) (Fig. 3B) $D(\mathrm{FI}) = \sqrt{((FI-334)/0.0151}$, supporting that the fluorescence intensity in combination with suitable sorted fluorophore-labeled calibrators can be used to estimate the size of unilamellar fluorophore-labeled liposomes. The fitted background level for our model ($b = 344$) is also in good agreement with our experimental threshold level that is based on a trigger value of 200 that was used to keep the rate of background events to less than two events/s. The *SD* of the FI-based size estimation corresponds to 44, 41, 44 nm for fraction F1, F2, and F3, respectively, when translating the *SD*(FI) of the fitted Gaussian functions shown in Figure 3A to *SD*(size(FI)) based on the *D*(*FI*) relation shown in Figure 3B. These values

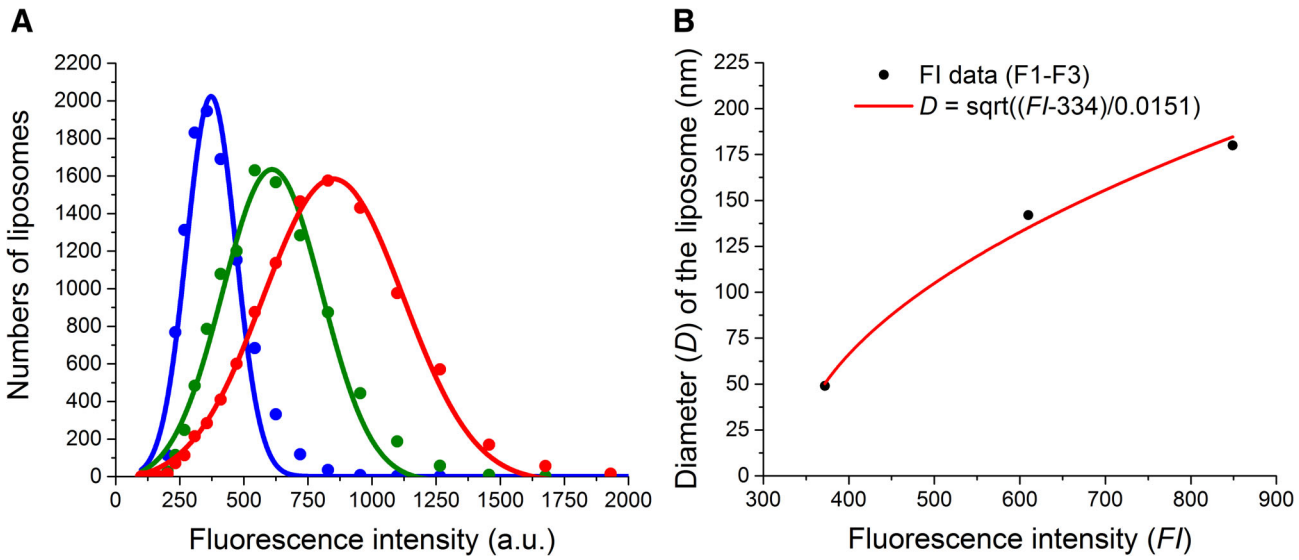

Figure 3. (**A**) The fluorescence intensity profile of the three different sorted liposome fractions on a linear scale (circles) and their corresponding Gaussian fits (solid lines). These data are also shown in Figure 1B on a log scale. (**B**) The NTA size (Gaussian mean diameter [*D*]) as a function of their corresponding fluorescence intensity (Gaussian mean [*FI*]) from flow cytometry including the fitted correlation between these two measures: $D = \sqrt{((FI-b)/k)}$, *b* refers to a background component and *k* a calibration factor.

are similar to the NTA-derived *SD*-values corresponding to 34 and 39 nm in the case of F2 and F3 fractions, respectively. The FANS-derived *SD* for F1 is notably higher than the corresponding *SD*-value derived from NTA (Table 1).

Next, we compared size distributions of a bulk (polydisperse) liposome solution derived from flow cytometry using the *D*(*FI*) equation with commonly used methodologies, NTA and cryo-TEM (see Figure 4). NTA and flow cytometry show good agreement, both reporting the most frequent size of the liposomes to be approximately 100 nm ± 50 nm. In contrast, cryo-TEM found the liposomes to be larger (distributed around 150 nm). However, the fairly low numbers of events (*n*) detected in the case of the NTA ($n = 322$) and in particular the Cryo-TEM ($n = 248$) may to some extent account for the discrepancies. Along these lines, the smooth black curve shown in Figure 4 highlights the high-throughput advances of flow cytometry compared to cryo-TEM and NTA.

Correlating the SSC of Liposomes with Size: A Challenge

Since SSC is more sensitive than FSC (11), this was employed to discriminate the three FANS-sorted liposome fractions. The coefficient of variation (CV = SD/mean value) is a relative measure of the resolution of the apparatus (including the size-heterogeneity) in terms of the broadness of the peak signal. The CV of the fluorescence intensity (FI) of fraction F1 and F3 are smaller than for the CV-value based on SSC—the SSC values are based on data shown in Figure 5: CV(SSC(F1)) = 0.44 and CV(FI(F1)) = 0.26, and CV(SSC(F3)) = 0.40 and CV(FI(F3)) = 0.32. Importantly, the SSC profile of the bare DPBS (sheath fluid) looks very similar to the SSC profiles of the liposomes fractions. Thus, the majority of the SSC signal seems to be associated with the background rather than the

Table 1. List of the different sizes and corresponding standard deviations based on the Gaussian analysis of the NTA- and flow cytometry/FI-derived data

SAMPLE/MEASURE[1]	SIZE (NTA)	*SD* (SIZE, NTA)	SIZE (FI)	*SD* (SIZE(FI))
Fraction 1 (F1)	49	12	50	44
Fraction 2 (F2)	142	34	135	41
Fraction 3 (F3)	180	39	185	44

[1] Sizes (diameter) and *SD* values are in nm.

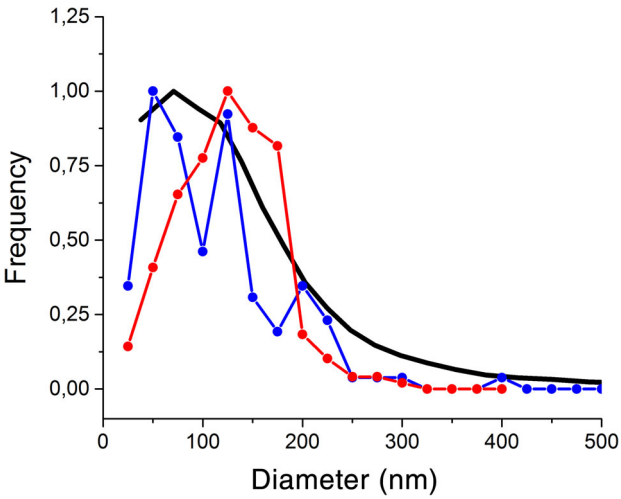

Figure 4. Normalized size distributions of the bulk (polydisperse) liposome solution based on flow cytometry using the fluorescence intensity in combination with our FANS-sorted calibrators (black features, number of particles (*n*) = 10,000), NTA (blue features, $n = 322$) and cryo-TEM (red features, $n = 248$). The size distribution derived from flow data is based on the conversion from fluorescence intensity to size as shown in Figure 3B.

weakly scattering liposomes. On this note, this work clearly illustrates that the resolution of SSC for our experimental setup is very low for liposomes in the size range (30–300 nm).

Discussion

Liposomes are submicron-sized particles (excl. giant vesicles) with a refractive index very close to water. Thus, in contrast with metallic nanoparticles, they exhibit a low scattering cross section. Since flow cytometers are designed to study cells and particles larger than 1 μm in diameter, a particle size around 100 nm pose a challenge. By inserting lipid-anchored fluorescent molecules into the liposome membrane, we, as a proof-of-principle, show that we are able to sort liposomes of different sizes and use the FANS-sorted liposomes to correlate fluorescence intensity from the liposomes obtained from flow cytometry with their estimated size. This was confirmed by NTA and cryo-TEM. A key requisite for correlating fluorescence intensity from the liposomes with size is the use of unilamelar liposomes. The described procedure facilitates this and was confirmed (Supporting Information Fig. S3).

Our sizing strategy relies on the fact that we could combine FANS sorting of liposomes and NTA to get actual size information of the very diluted FANS-sorted liposome fractions. We have previously described a method to use liposomes as size calibrators for microvesicles that relied on several assumptions including that the largest size population of the flow cytometric detected liposomes was equal to the size of the pore membrane used for extruding the liposomes (4). In this work, we significantly improve our size estimation by correlating the flow cytometry intensities with size values of our FANS calibrators obtained from NTA (Fig. 2). Nolan et al. (8) studied extruded liposomes using flow cytometry and NTA data. They obtained a very good agreement between the NTA sizes and the fluorescent intensities for extruded liposomes around 100 nm. However, for the larger liposomes (liposomes extruded through 200 nm pores), they observed discrepancies. These differences between size and fluorescence intensities could be due to the presence of multilamellar liposomes and/or that the partitioning coefficient of the post-inserted fluorophore could depend on the surface curvature of the liposomes (26). In our work, we study a polydisperse liposome sample and confirm that our flow cytometric method for estimating the liposome size distribution of polydisperse liposomes is in fairly good agreement with results obtained from NTA and cryo-TEM (Fig. 4). Additionally, we show that the SSC readout from 30 to 300 nm-sized liposomes is comparable to the SSC readout from the DPBS background (Fig. 5) and thus, at least for the standard apparatus to our disposal, did not represent a viable option for size estimation.

Our data are in full agreement with previous fluorescence-microscopy studies showing that the fluorescence intensity of individual liposomes scales directly with the area of the liposome meaning that the diameter is proportional to the square root of FI (Fig. 3) (4,25). Although the reanalyzed sorted FANS fractions deviated from the gates used to sort them (Fig. 1B). We suggest that this discrepancy could be due to that some of

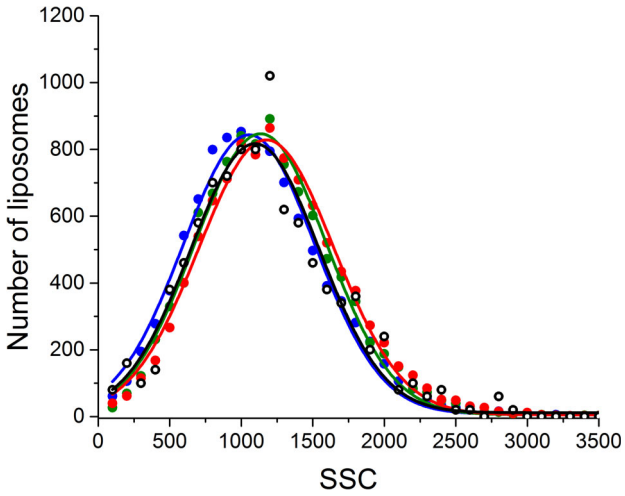

Figure 5. The SSC profiles of the three sorted liposome fractions. The solid blue, green, and red dots represent the F1, F2, and F3 data, respectively. The corresponding Gaussian fits are also shown using the same color codes (lines). The SSC data of the bare DPBS are also shown (black circles) including the Gaussian fit (black line).

the larger liposomes and liposome components may adsorb to the surface of the vial used for sorting. To support this, we learned during the studies that low-protein-binding Eppendorf tubes gave rise to a larger shift in FI (relative to the sorting gates) compared to the Falcon round-bottom polystyrene tubes that were used in this work. Moreover, the flow cytometer performance/accuracy could change slightly between the sorting and the analysis of the sorted fractions. That said, we exclude that co-particle events during the sorting process give rise to the shift. If co-particle events were a big issue during the sorting, a background population of the most abundant size of liposomes in the bulk sample (~100 nm) (Fig. 4) would be expected in the NTA data of the different fractions. According to Figure 2 we do not observe that. Nevertheless, these data still show, for the first time, that unilamellar liposomes can be sorted using flow cytometric sorting, giving rise to fairly distinct size populations that can subsequently be used for calibrating fluorescent intensity to liposome size. It should be stressed that liposomes typically exhibit a mean size of around 100–200 nm (25). Thus, well-defined sizes of liposomes above these values are very difficult to obtain. Normally extrusion is applied to form "well-defined" liposomes sizes, but, in general, the most abundant liposome size (~100–200 nm) is typically not changed significantly when applying pore-membrane sizes above 100–200 nm for extrusion ((23), see Supporting Information). These inherent limitations in the control of the mean size of liposomes (above 100–200 nm) makes it difficult to prepare different well-defined sizes of liposomes for calibrations and thus highlights the uniqueness of our FANS-sorted size populations.

We obtained good agreement between FANS-derived sizes *SD* values and NTA-derived values (Table 1). This was particularly evident for the larger fractions (F2 and F3), whereas the smallest and most dim particles (fraction F1)

gave rise to a relatively broad feature (relative to its mean) because of the poor counting statistics (27) in addition to the broadening effect due to the log-scale. It should be noted that the *SD* values contain contributions from the real size-heterogeneity in the sample/fraction and the size-resolution of the technique. However, the discrepancy between *SD* values obtained from different techniques of the same sample/fraction should thus reflect the different size resolution of the different techniques in relative terms. The flow cytometric resolution based on the fluorescence of liposomes could be improved by increasing the fluorescent signal using a larger mole percent of fluorophores in the liposomes, with the limitation that too many fluorophores may alter the structure of the liposomes or give rise to self-absorption/quenching effects. Advancing the sensitivity of flow cytometers would also improve the flow cytometric size resolution associated with the use of our FANS-derived size calibrators. In general, the resolution in terms of *SD* values obtained from the *FI*-flow cytometry evaluation of the FANS-sorted fractions was comparable with the corresponding *SD* values derived from NTA.

Cryo-TEM is the golden standard to assess liposome size. Yet, when analyzing liposomes with a large variation in size a potential bias toward the detection of larger liposomes is possible. One reason for this is that fields of view are not completely randomly chosen and another reason is that the smallest liposomes can be difficult to resolve. The size distribution derived from NTA (Fig. 4) seems to match the *FI*-derived size profile quite well and thereby support that our FANS-based methodology is valid to estimate the size of individual liposomes with a high-throughput.

The scattering output can also be used to estimate the size of many unlabeled nanoparticles (2,4,13). The Mie scattering theory that describes the scattering properties of spherical nanoparticles with a size comparable to the wavelength used to probe the particles (13) is however far more complex than the simple radius-squared relation between the size of liposomes and their corresponding fluorescence intensity (4,25). Thus, using reliable size calibrators seems to be a valid and robust approach to get information about sizes from the scattering output. Hence, by sorting several fractions according to the SSC of different sizes of nanoparticles, well-defined size bins can be defined and used to provide a size distribution of nanoparticles based on the flow cytometric scattering readout, similar to the FANS procedure presented herein. While more sensitive SSC and/or FSC detection setups than the FACSAria setup used in this study may provide scattering output useful for vesicle size determination (12,13), we find that the SSC resolution to be limited for small (30–300 nm) liposomes. This is highlighted by the SSC profile of the bare DPBS solution looking very similar to the SSC profiles of the liposomes fractions (Fig. 5), suggesting that the majority of the SSC signal is associated with the background rather than the weakly scattering liposomes.

The Potential Use of Flow-Activated Nanoparticle-Sorted Calibrators Beyond Liposomes

We propose that our applied strategy, which combines FANS sorting with NTA, provides proper calibrators for characterizing the size of unilamellar liposomes and other types of spherical nanoparticles such as extracellular vesicles, metallic, and polymeric nanoparticles. Opposite to liposomes, metallic nanoparticles exhibit a high scattering cross section. Thus, a polydisperse sample of spherical metallic particles can be evaluated by conventional flow cytometry including sorting and NTA. It has recently been shown (1) that conventional flow cytometry combined with sorting could quantify and sort gold nanoparticle dimers from a complex mixture of different types of gold nanoparticle oligomers. However, since locating the gold nanoparticles was challenging using TEM at this low concentration, we recommend using NTA for the analysis of the sorted samples, with its much higher throughput compared to traditional TEM.

The need for assessing the size of EV populations detected by flow cytometry has been repeated several times the past few years (14,18–20). In principle, liposomes could be used as calibrators for EV size determination due to the structural similarity between liposomes and EVs (both are core–shell structure), instead of using solid plastic and silica beads that are traditionally used as EV size calibrators. To further enhance the similarity between liposomes and EVs, the liposomes could be loaded with sorbitol or sugars to better match the refractive index of the core of the EVs. Yet, EVs are a very heterogeneous population of biological nanoparticles when it comes to size and composition and therefore also refractive indexes. On that note, it should also be stressed that isolated plasma-derived EVs are highly prone to contamination with highly abundant lipoproteins (28,29). Recent work (12) shows that by taking the ratio between SSC and FSC (they used a high scatter sensitivity flow cytometer) in combination with Mie scattering theory, EV sizes in the range from 200 to 500 nm could be deduced. However, the solid-sphere model does not take into account that EVs have a hollow structure comprised several refractive indexes and interfaces that may be important to add to the description of the scattering cross section of EVs. To confirm the validity of combining Mie scattering theory and the scatter readouts to assess the size of EVs using flow cytometry, we propose the following strategy. FANS-sorted EVs according to their scatter intensity to verify whether the EV size based on the scatter signals and Mie-theory are in agreement with the real size obtained from the NTA measurements of the FANS-sorted EV fractions. That said, the need for both an NTA and FACS machine may challenge the practical use of the FANS-sorted size-calibrator strategy.

Conclusions

This work shows, for the first time, that well-defined sizes of liposomes can be sorted using FANS sorting. This finding allowed us, as a proof-of-principle, to correlate the flow cytometric fluorescence and SSC intensity readouts with the size of liposomes by using FANS-sorted calibrators sized by NTA. By doing so, our data based on the fluorescence readout followed the theoretically predicted size dependency and thus enabled us to convert the fluorescent readout of all liposomes measured in the flow cytometric setup to estimated liposome

size. Furthermore, we benchmarked and validated the size distribution of a polydisperse liposome sample derived from flow cytometry in combination with the FANS calibrators against standard methods for sizing nanoparticles including NTA and cryo-TEM and obtained comparable size distributions.

We propose that the FANS-sorted liposomes provides an alternative method to estimate the size of liposomes using flow cytometry that relies on unique calibrators that exhibit sizes, structures, and refractive indexes that are identical to the particles being studied.

Our study also demonstrated the poor resolution of the scattering readout and a significantly better resolution of the fluorescence signal when using these flow cytometric readouts to estimate the size of nano-sized liposomes loaded with 1 mol % atto488-DOPE. That said, it should be noted that the sensitivity of both the scattering and emission (30) varies between flow cytometers.

Finally, it should be highlighted that typically flow cytometers exhibit highly attractive properties such as a linear dynamic range from 3 to 7 decades, multiparameter-analysis and high-throughput information at a single-particle level. Thus, further efforts on advancing this technique for nanoparticle characterization would be highly appreciated in many areas of nanoparticle-based research. This work adds a new method for size estimation to the list of properties that flow cytometry can assess by combining FACS-sorting with NTA. However, advancement in the sensitivity of conventional flow cytometers in general is needed to improve the size determination based on either scattering or fluorescence intensity even further.

Acknowledgments

We would like to thank Lundbeck Foundation Research Initiative on Brain Barriers and Drug Delivery (Grant no. R155-2013-14113) and Novo Nordisk Foundation (Grant no. NNF16OC0022166) for financial support to this project. J.B.S. would like to thank Novo Nordisk Foundation (Grant no. NNF17OC0028262) for support. J.B.L would like to acknowledge support from the Sapere Aude program under the Danish Council for Independent Research. We would also like to thank John P. Nolan, Thomas C. B. Klauber and Paul Kempen for valuable discussions.

Literature Cited

1. Simonsen JB, Reeler NEA, Fossum A, Lerstrup KA, Laursen BW, Nørgaard K. Quantifying and sorting of gold nanoparticle dimers from complex reaction mixtures using flow cytometry. Nano Res 2016;9:3093–3098.
2. Zhu S, Ma L, Wang S, Chen C, Zhang W, Yang L, Hang W, Nolan JP, Wu L, Yan X. Light-scattering detection below the level of single fluorescent molecules for high-resolution characterization of functional nanoparticles. ACS Nano 2014;8:10998–11006.
3. Zucker RM, Ortenzio JNR, Boyes WK. Characterization, detection, and counting of metal nanoparticles using flow cytometry. Cytom. Part A 2016;89:169–183.
4. Simonsen JB. A liposome-based size calibration method for measuring microvesicles by flow cytometry. J Thromb Haemost 2016;14:186–190.
5. Temmerman K, Nickel W. A novel flow cytometric assay to quantify interactions between proteins and membrane lipids. J Lipid Res 2009;50:1245–1254.
6. Vorauer-Uhl K, Wagner A, Borth N, Katinger H. Determination of liposome size distribution by flow cytometry. Cytometry 2000;39:166–171.
7. Chen C, Zhu S, Wang S, Zhang W, Cheng Y, Yan X. Multiparameter quantification of liposomal nanomedicines at the single-particle level by high-sensitivity flow cytometry. ACS Appl Mater Interfaces 2017;9:13913–13919.
8. Stoner SA, Duggan E, Condello D, Guerrero A, Turk JR, Narayanan PK, Nolan JP. High sensitivity flow cytometry of membrane vesicles. Cytom Part A 2016;89:196–206.
9. Arraud N, Gounou C, Turpin D, Brisson AR. Fluorescence triggering: A general strategy for enumerating and phenotyping extracellular vesicles by flow cytometry. Cytom. Part A 2016;89:184–195.
10. Lannigan J, Nolan JJ, Zucker R. Measurement of extracellular vesicles and other submicron size particles by flow cytometry. Cytom. Part A 2016;89:109–110.
11. Poncelet P, Robert S, Bailly N, Garnache-Ottou F, Bouriche T, Devalet B, Segatchian JH, Saas P, Mullier F. Tips and tricks for flow cytometry-based analysis and counting of microparticles. Transfus Apher Sci 2015;53:110–126.
12. van der Pol E, de Rond L, Coumans FAW, Gool EL, Böing AN, Sturk A, Nieuwland R, van Leeuwen TG. Absolute sizing and label-free identification of extracellular vesicles by flow cytometry. Nanomedicine 2018;14:801–810.
13. van der Pol E, Coumans FAW, Grootemaat AE, Gardiner C, Sargent IL, Harrison P, Sturk A, van Leeuwen TG, Nieuwland R. Particle size distribution of exosomes and microvesicles determined by transmission electron microscopy, flow cytometry, nanoparticle tracking analysis, and resistive pulse sensing. J Thromb Haemost 2014;12:1182–1192.
14. Chandler WL, Yeung W, Tait JF. A new microparticle size calibration standard for use in measuring smaller microparticles using a new flow cytometer. J Thromb Haemost 2011;9:1216–1224.
15. van der Vlist EJ, Nolte-'t Hoen ENM, Stoorvogel W, Arkesteijn GJA, Wauben MHM. Fluorescent labeling of nano-sized vesicles released by cells and subsequent quantitative and qualitative analysis by high-resolution flow cytometry. Nat Protoc 2012;7:1311–1326.
16. Properzi F, Logozzi M, Fais S. Exosomes: The future of biomarkers in medicine. Biomark Med 2013;7:769–778.
17. Johnsen KB, Gudbergsson JM, Skov MN, Pilgaard L, Moos T, Duroux M. A comprehensive overview of exosomes as drug delivery vehicles - endogenous nanocarriers for targeted cancer therapy. Biochim Biophys Acta - Rev Cancer 2014;1846:75–87.
18. Robert S, Poncelet P, Lacroix R, Raoult D, Dignat-George F. More on: Calibration for the measurement of microparticles: Value of calibrated polystyrene beads for flow cytometry-based sizing of biological microparticles. J Thromb Haemost 2011;9:1676–1678.
19. Maas SLN, De Vrij J, Van Der Vlist EJ, Geragousian B, Van Bloois L, Mastrobattista E, Schiffelers RM, Wauben MHM, Broekman MLD. Nolte-'T Hoen ENM. Possibilities and limitations of current technologies for quantification of biological extracellular vesicles and synthetic mimics. J Control Release 2015;200:87–96.
20. Mullier F, Bailly N, Chatelain C, Dogné JM, Chatelain B. More on: Calibration for the measurement of microparticles: Needs, interests, and limitations of calibrated polystyrene beads for flow cytometry-based quantification of biological microparticles. J Thromb Haemost 2011;9:1679–1681.
21. Li C, Deng Y. A novel method for the preparation of liposomes: Freeze drying of monophase solutions. J Pharm Sci 2004;93:1403–1414.
22. Schindelin J, Arganda-Carreras I, Frise E, Kaynig V, Longair M, Pietzsch T, Preibisch S, Rueden C, Saalfeld S, Schmid B, et al. Fiji: An open-source platform for biological-image analysis. Nat Methods 2012;9:676–682.
23. Hatzakis NS, Bhatia VK, Larsen J, Madsen KL, Bolinger PY, Kunding AH, Castillo J, Gether U, Hedegård P, Stamou D. How curved membranes recruit amphipathic helices and protein anchoring motifs. Nat Chem Biol 2009;5:835–841.
24. Larsen J, Hatzakis NS, Stamou D. Observation of inhomogeneity in the lipid composition of individual nanoscale liposomes. J Am Chem Soc 2011;133:10685–10687.
25. Kunding AH, Mortensen MW, Christensen SM, Stamou D. A fluorescence-based technique to construct size distributions from single-object measurements: Application to the extrusion of lipid vesicles. Biophys J 2008;95:1176–1188.
26. Larsen JB, Jensen MB, Bhatia VK, Pedersen SL, Bjørnholm T, Iversen L, Uline M, Szleifer I, Jensen KJ, Hatzakis NS, et al. Membrane curvature enables N-Ras lipid anchor sorting to liquid-ordered membrane phases. Nat Chem Biol 2015;11:192–194.
27. Chase ES, Hoffman RA. Resolution of dimly fluorescent particles: A practical measure of fluorescence sensitivity. Cytometry 1998;33:267–279.
28. Simonsen JB. What are we looking at? Extracellular vesicles, lipoproteins, or both? Circ Res 2017;121:920–922.
29. Johnsen KB, Gudbergsson JM, Andresen TL, Simonsen JB. What is the blood concentration of extracellular vesicles? Implications for the use of extracellular vesicles as blood-borne biomarkers of cancer. BBA Rev Cancer 2019;1871:109–116.
30. Parks DR, El Khettabi F, Chase E, Hoffman RA, Perfetto SP, Spidlen J, Wood JCS, Moore WA, Brinkman RR. Evaluating flow cytometer performance with weighted quadratic least squares analysis of LED and multi-level bead data. Cytom. Part A 2017;91:232–249.